

## Observation of Brownian Motion on the Time Scale of Hydrodynamic Interactions

M. H. Kao and A. G. Yodh

*Department of Physics, University of Pennsylvania, Philadelphia, Pennsylvania 19104*

D. J. Pine

*Exxon Research and Engineering Co., Route 22 East, Annandale, New Jersey 08801*

(Received 22 September 1992)

We resolve the mean square displacement of particles in concentrated suspensions during the first 20 ns of their motion, before hydrodynamic interactions between particles have had time to fully develop. Nevertheless, we find that the concentrated systems exhibit clear deviations from the isolated-particle theory. These deviations are well described by several scaled versions of the isolated-particle theory. The measurements also demonstrate a new multiple-scattering photon correlation technique with ultrashort time resolution.

PACS numbers: 82.70.Dd, 05.40.+j, 66.20.+d, 82.70.Kj

The Brownian motion of particles in a fluid is a problem with spectacular historical roots [1] that continues to provide us with intriguing new physics. Most recently there has been renewed interest in the *first steps* of these motions [2-5]. This is largely a result of new experimental probes [4, 6] that enable us to measure particle displacements down to 1 Å, and thereby offer the possibility to quantitatively test hydrodynamic theories [2, 3] of nondiffusive particle motion.

Perhaps the simplest possible Brownian system is composed of an *isolated* spherical particle of radius  $a$  in an infinite, incompressible fluid with density  $\rho$  and viscosity  $\eta$ . A full hydrodynamic treatment of this problem [3] reveals that a Brownian particle will persist in a given direction of motion until the fluid momentum (or vorticity) generated by the Brownian particle diffuses away. This leads to a slow power-law decay of the particle velocity autocorrelation function characterized by a hydrodynamic time scale,  $\tau_\nu^0 = \rho a^2 / \eta$ , which corresponds to the time it takes the vorticity to diffuse a particle radius. Purely diffusive particle motion sets in on time scales of  $10^3 \tau_\nu^0$ . In any real suspension, however, particles are not isolated but are coupled via hydrodynamic forces. While substantial work has been devoted to the diffusive motion of interacting particles on long time scales, at present there is little understanding of the nondiffusive motions of interacting particles at very short time scales.

In this work we resolve the mean square displacement  $\langle \Delta r^2(\tau) \rangle$  of particles in concentrated hard-sphere suspensions during the first 20 ns of their motion. These are the shortest time scales ever probed in the study of Brownian dynamics. The measurements reveal the influence of transient hydrodynamic interactions on time scales of the order  $\tau_\nu^0$  and substantially shorter. Our measurements encompass three particle sizes and particle volume fractions  $\phi$  of up to 0.24. We find that the dilute systems follow the isolated-particle theory [3] down to approximately  $\tau_\nu^0/10$ . However, over these same time scales, the concentrated systems exhibit clear deviations from the

isolated-particle theory. This latter result is particularly surprising since even in our most concentrated samples, the mean distance between adjacent particle surfaces is comparable to or greater than the particle radius. In this limit, one might expect that there would be insufficient time for hydrodynamic interactions between particles to be significant. Furthermore, an intriguing scaling with concentration that has been observed on time scales longer than  $\tau_\nu^0$  [5] appears to describe our data at times substantially shorter than  $\tau_\nu^0$ . We find, however, that our observations can also be described by other scaled versions of the isolated-particle theory. The present measurements also provide an important experimental test of a new lattice-Boltzmann simulation scheme [7] and introduce a new class of correlation experiment which combines diffusing-wave spectroscopy (DWS) [6] with Michelson interferometry to yield electric field temporal autocorrelation functions on nanosecond and subnanosecond time scales [8].

The first part of our experimental apparatus [see Fig. 1(a)] utilizes standard DWS techniques [6]. Sample cells containing suspensions of polystyrene spheres in water were illuminated from one side by the 514-nm line of a cw Ar-ion laser and a single speckle of transmitted light was monitored. To obtain mean square particle displacements on nanosecond time scales, we have made a novel modification. We replaced the electronic photon correlator with a 3-m Michelson interferometer. The sample speckle field is divided at the interferometer entrance, directed along two spatially separated paths of differing length, and then recombined on a light detector. In this case the time-averaged intensity we measure  $\langle I(\tau) \rangle$  depends on the temporal delay  $\tau$  introduced between the recombined fields, the optical carrier frequency  $\omega$ , the average speckle intensity  $I_{\text{ave}}$ , and the temporal autocorrelation function  $g_1(\tau) = |\langle E^*(t+\tau)E(t) \rangle| / \langle |E(t)|^2 \rangle$  of the sample speckle field, i.e.,

$$\langle I(\tau) \rangle = \frac{1}{2} I_{\text{ave}} [1 + g_1(\tau) \cos(\omega\tau)]. \quad (1)$$

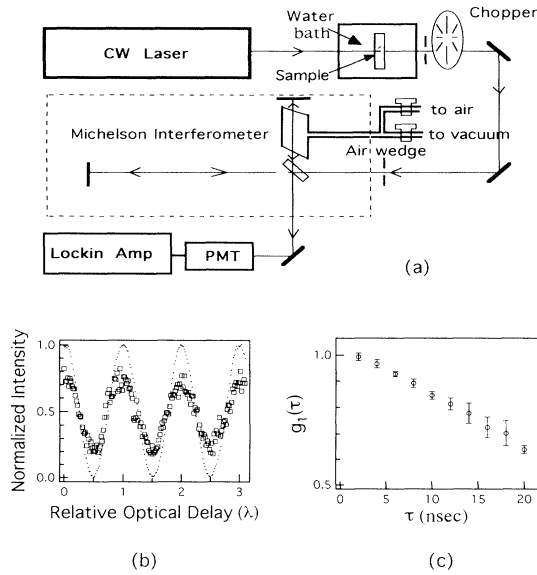


FIG. 1. (a) Experimental setup. Coarse delays are implemented by moving the long interferometer arm. Fine delays are achieved by changing the partial pressure of the air wedge in the short arm. (b) Normalized scanning fringes at  $\tau = 0$  ns (solid dots) and  $\tau = 20$  ns (squares) for  $\phi = 0.0385$ ,  $0.299\text{-}\mu\text{m}$ -diam polystyrene suspension. The vertical axis is the normalized light intensity measured on the lock-in amplifier. The effects of laser coherence and geometry were normalized using a dilute sample that did not decay on the time scales probed. (c) A single run of  $g_1(\tau)$  vs  $\tau$  for the same suspension.

Thus, the temporal visibility of the detected intensity directly yields  $g_1(\tau)$ . Our new method overcomes several limitations inherent in conventional photon correlation methodologies. The time resolution is at least 10 times better than the smallest commercially available correlator bin width and can in principle be as short as a few femtoseconds; the minimum count rates can be lower than 1 kHz without degrading the signal-to-noise ratio, and in contrast to DWS intensity correlation measurements [9], the information derived from the *electric field* correlation function is not affected when the laser coherence length becomes smaller than the typical photon path length through the medium.

In Fig. 1(b) we show two normalized visibility curves taken at delays of  $\tau = 0$  and 20 ns. The amplitude decay of these oscillations reflects the particle motions. We determined these amplitudes in 1-ns intervals by the coarse movement of one arm in the interferometer. The decay of visibility, i.e.,  $g_1(\tau)$ , during one experimental run is shown in Fig. 1(c). We determined  $g_1(\tau)$  for samples of  $0.205\text{-}$ ,  $0.299\text{-}$ , and  $0.460\text{-}\mu\text{m}$ -diam polystyrene spheres in water for volume fractions  $\phi$  ranging from 0.02 to 0.24. By adding an appropriate amount of HCl to the suspension, the particle screening length was kept below  $50\text{ \AA}$ , thereby ensuring that the direct interactions were essentially hard sphere. The sample cells were immersed in

water in order to maintain the sample temperatures at  $24^\circ\text{C}$  and minimize reflections at the sample walls.

For weakly interacting but multiply scattering particle suspensions, DWS theory gives [6]

$$g_1(\tau) = \int_0^\infty P(s) e^{-\frac{1}{2}k_0^2 \langle \Delta r^2(\tau) \rangle s/l^*} e^{-s/l_a} ds. \quad (2)$$

Here  $k_0$  is the wave vector of light in the medium,  $l^*$  is the photon random walk step length [6],  $l_a$  is the light absorption length in the medium, and  $P(s)$  represents the probability that a photon travels a distance  $s$  through the medium before emerging at the detection point. The spatial resolution of the measurement is set by the typical path length of a diffusing photon. In order to resolve displacements less than  $1\text{ \AA}$ , this path length must be several meters. Thus, the experiment required very thick sample cells (1 to 3 cm) and we had to systematically account for the effects of absorption and geometry in these samples. We independently determined  $l^*$  for each of our samples by static transmission and by long-time diffusion measurements using conventional DWS on millimeter-thick samples. The DWS measurements were typically within 5% of our calculations of  $l^*$  from Mie theory, but were exceedingly accurate ( $\sim 1\%$  variation) and were prone to fewer systematic errors than either the static transmission measurements or the theoretical estimates which require accurate knowledge of sample material properties. We computed  $P(s)$  analytically for our cylindrical cells [10] and included the effects of light loss through the cell walls as well as the exact illumination and detection geometries. Finally we performed absolute transmission measurements as a function of cell thickness which, along with our measured  $l^*$  and calculated  $P(s)$ , enabled us to deduce  $l_a$  (1–5 m). Using this information and our measured  $g_1(\tau)$ , we determined  $\langle \Delta r^2(\tau) \rangle$  by inverting Eq. (2).

For volume fractions of a few percent and lower,  $\langle \Delta r^2(\tau) \rangle$  is accurately obtained from the measured  $g_1(\tau)$  using Eq. (2). At higher concentrations, however, interactions become important and the measured  $g_1(\tau)$  can also contain contributions from density fluctuations involving more than one particle, particularly if the mean interparticle distance is less than the wavelength of light. In this case, the quantity  $\langle \Delta r^2(\tau) \rangle$  in Eq. (2) must be replaced by

$$\{ \langle \Delta r^2(\tau) \rangle + [A(q, \tau)] \} / [S(q)], \quad (3)$$

where  $S(q)$  is the structure factor of the suspension and  $A(q, \tau) = \frac{1}{N} \sum_{i \neq j}^N \langle \Delta \mathbf{r}_i(\tau) \cdot \Delta \mathbf{r}_j(\tau) e^{i\mathbf{q} \cdot [\mathbf{r}_i(0) - \mathbf{r}_j(0)]} \rangle$  is a time- and  $q$ -dependent factor which accounts for the correlated motions and scattering of different particles [11]. The square brackets denote the  $q$  average,  $[X] = \int_0^{2k_0 a} X(q) F(q) q^3 dq / \int_0^{2k_0 a} F(q) q^3 dq$ , where  $F(q)$  is the particle form factor. The structural correction  $[S(q)]$  is easily computed within the Percus-Yevick [12] approximation and works very well for hard spheres at these volume fractions. The quantity  $[A(q, \tau)]$  has been

calculated for hard spheres at long times when the particles are moving diffusively [13]. In the long time limit,  $[A(q, \tau)]$  is  $\sim 6$  times smaller than  $\langle \Delta r^2(\tau) \rangle$  for our most concentrated sample of 0.205- $\mu\text{m}$ -diam spheres. The correction factor rapidly diminishes with both increasing particle size and decreasing volume fraction.  $[A(q, \tau)]$  has not been calculated at short times, but must vanish as  $\tau$  approaches zero. Our data span both dilute and concentrated regimes. In our analysis we have assumed  $[A(q, \tau)]$  is zero, but we have included the structural correction. We will reexamine the possible violation of this approximation towards the conclusion of the paper.

In Fig. 2, we show the time-dependent rms displacement,  $\sqrt{\langle \Delta r^2(\tau) \rangle}$ , of 0.205- $\mu\text{m}$ -diam particles at two different concentrations. Data from the lowest concentration sample,  $\phi = 0.02$ , are in excellent agreement with the isolated-particle theory [3]. We emphasize that there are no adjustable or calculated experimental parameters in making this comparison. These results confirm the validity of the hydrodynamic theory down to times much less than the characteristic hydrodynamic time  $\tau_\nu^0$  (12.5 ns for this sample). At higher concentrations, the data exhibit systematic departures from the isolated-particle theory. At a given delay time  $\tau$ , the rms displacement of a particle decreases with increasing volume fraction consistent with the expectation that hydrodynamic interactions with neighboring particles effectively impede particle motion. We have observed these effects in all our concentrated samples on time scales significantly less than the time it takes the fluid momentum to diffuse the *mean* distance between nearest-neighbor particle surfaces. The measurements suggest that *average particle motion* is still modified by hydrodynamic interactions, but that these interactions arise only occasionally between particles whose distance of closest approach is substantially smaller than the mean particle separation.

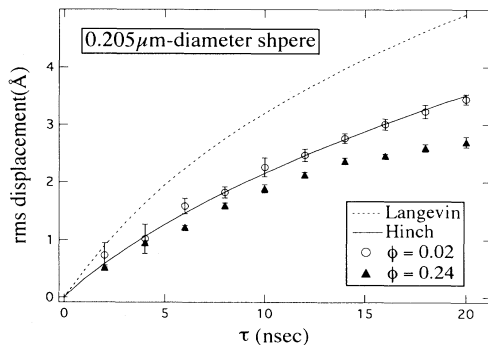


FIG. 2. The rms displacement  $\sqrt{\langle \Delta r^2(\tau) \rangle}$  vs  $\tau$  of 0.205- $\mu\text{m}$ -diam polystyrene spheres in water at two different volume fractions. The solid line is the isolated-particle theory of Hinch. The dashed line is the prediction of simple Langevin theory that includes only Stokes drag. The concentrated suspension clearly shows measurable deviations from the isolated-particle theory.

Recent experiments [5] and simulations [7] suggest that the time evolution of Brownian particles in concentrated suspensions obeys a remarkable scaling with respect to the isolated-particle theory. Briefly, the isolated-particle theory predicts  $\langle \Delta r^2(\tau) \rangle = 6D_0\tau_\nu^0 f(\tau/\tau_\nu^0)$ , where  $D_0 = kT/6\pi a\eta$  is the Stokes-Einstein diffusion coefficient, and  $f(\tau/\tau_\nu^0)$  is an algebraic function [3]. Scaling is accomplished by replacing  $D_0$  and  $\tau_\nu^0$  with the  $\phi$ -dependent functions  $D(\phi)$  and  $\tau_\nu(\phi)$ . In Fig. 3 we investigate three different scaling schemes. In each graph we plot a scaled rms displacement,  $\{\langle \Delta r^2(\tau) \rangle / 6D(\phi)\tau_\nu(\phi)\}^{1/2}$ , as a function of a scaled time  $\tau/\tau_\nu(\phi)$ . The first scheme, originally proposed by Zhu *et al.* [5] to explain volume fraction dependent measurements on time scales greater than  $\tau_\nu^0$ , sets  $D(\phi) = D_s(\phi) = D_0(1 - 1.83\phi)$  and  $\tau_\nu(\phi) = \rho a^2 / \eta_{\text{HF}}(\phi)$ , where  $\eta_{\text{HF}}(\phi)$  is the high frequency viscos-

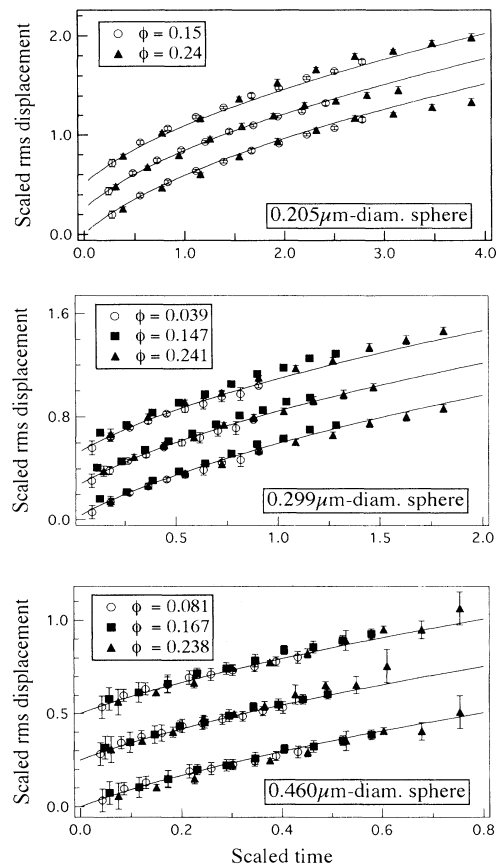


FIG. 3. Scaled rms displacement  $\{\langle \Delta r^2(\tau) \rangle / 6D(\phi) \times \tau_\nu(\phi)\}^{1/2}$  vs scaled time  $\tau/\tau_\nu(\phi)$ . In each graph, the three scaling theories are shown (see text). The lower set of data is scaled by  $D(\phi) = (1 - 1.83\phi)D_0$  and Beenakker's  $\tau_\nu(\phi) = \rho a^2 / \eta_{\text{HF}}(\phi)$ ; the middle set by  $D(\phi) = (1 - 1.83\phi)D_0$  and  $\tau_\nu(\phi) = \tau_\nu^0(1 - 1.83\phi)$ ; the upper set by  $D(\phi) = kT/6\pi a\eta_{\text{HF}}(\phi)$  and  $\tau_\nu(\phi) = \rho a^2 / \eta_{\text{HF}}(\phi)$ . The solid lines represent the square root of the isolated-particle function, i.e.,  $f(\tau/\tau_\nu(\phi))$ . The data are displaced for clarity.

ity of the suspension calculated by Beenakker [14]; in the second scheme,  $D(\phi) = D_s(\phi)$  again, but we scale time according to  $\tau_\nu(\phi) = \tau_\nu^0(1 - 1.83\phi)$ ; in the third scheme we modify only the viscosity, i.e.,  $D(\phi) = kT/6\pi a\eta_{\text{HF}}(\phi)$  and  $\tau_\nu(\phi) = \rho a^2/\eta_{\text{HF}}(\phi)$ . It is apparent from the figure that all scaling schemes adequately describe the data over the full range of concentrations explored for each sample. Moreover, each of the scaling analyses provides a significantly better description of the data than does the unscaled isolated-particle theory of Hinch. A particularly interesting scenario is provided by the first scaling analysis. Zhu *et al.* interpreted the scaling as evidence that a Brownian particle moves in an effective medium which has the viscosity of the bulk suspension. It is surprising, therefore, that this same scaling analysis works at such short times since a particle cannot sense the effective viscosity of the bulk suspension for time scales much less than  $\tau_\nu^0$ . Our analysis enlarges the range of viable scaling schemes, and suggests that although the scaling of Zhu *et al.* appears valid for  $\tau > \tau_\nu^0$ , another scaling may underlie the behavior when  $\tau < \tau_\nu^0$ . Further work is needed to clarify this issue.

Finally, we return to reconsider our earlier assumption that the factor  $[A(q, \tau)]$  can be neglected in comparison to  $\langle \Delta r^2(\tau) \rangle$  in Eq. (3). If  $[A(q, \tau)] \ll \langle \Delta r^2(\tau) \rangle$ , then all the data we present are properly interpreted as the mean square displacement of a tracer particle. This hypothesis is supported by the observation that all of our results are well described by the scaling analysis, with the possible exception of our longest-time data for our smallest spheres. By contrast, it is possible that some of the measured deviation of the data from the isolated-particle theory arises as a result of non-negligible correlated scattering from different particles. In this case, the *time* dependence of the deviation implies that the motion of *different* particles is correlated for  $\tau < \tau_\nu^0$  and that these correlations are *changing* over these same time scales as a result of time-dependent hydrodynamic interactions. Thus, regardless of our assumption about  $[A(q, \tau)]$ , the data clearly imply that there are significant time-dependent hydrodynamic interactions between different particles which affect particle motion on time scales less than  $\tau_\nu^0$ . This surprising result presents a chal-

lenge to our current theoretical understanding of many-body hydrodynamic interactions between Brownian particles. In the future, lattice-Boltzmann computer simulations and  $q$ -dependent DWS experiments may provide new insight into these issues.

We thank Tony Ladd for valuable discussions and for sharing the results of his simulations prior to publication. We also acknowledge useful discussions with Peter Kaplan, Tom Lubensky, Dave Weitz, and James Lawler. This research is supported by the NSF through Grant No. DMR-9003687. A.G.Y. acknowledges partial support from the NSF through the PYI program, and from the Alfred P. Sloan Foundation.

- 
- [1] R. Brown, *Philos. Mag.* **4**, 161(1828); A. Einstein, *Ann. Phys. (Leipzig)* **17**, 549 (1905); **19**, 371 (1906).
  - [2] B. J. Alder and T. E. Wainwright, *Phys. Rev. A* **1**, 18 (1970); R. Zwanzig and M. Bixon, *J. Fluid Mech.* **69**, 21 (1975).
  - [3] E. J. Hinch, *J. Fluid Mech.* **72**, 499 (1975).
  - [4] D. A. Weitz, D. J. Pine, P. N. Pusey, and R. J. A. Tough, *Phys. Rev. Lett.* **63**, 1747 (1989).
  - [5] J. X. Zhu, D. J. Durian, J. Müller, D. A. Weitz, and D. J. Pine, *Phys. Rev. Lett.* **68**, 2559 (1992).
  - [6] G. Maret and P. E. Wolf, *Z. Phys. B* **65**, 409 (1987); M. J. Stephen, *Phys. Rev. B* **37**, 1 (1988); D. J. Pine, D. A. Weitz, J. X. Zhu, and E. Herbolzheimer, *J. Phys. (Paris)* **51**, 2101 (1990).
  - [7] A. J. C. Ladd (to be published).
  - [8] A. G. Yodh, N. Georgiades, and D. J. Pine, *Opt. Commun.* **83**, 56 (1991).
  - [9] P. E. Wolf and G. Maret, in *Scattering in Volumes and Surfaces*, edited by M. Nieto-Vesperinas and J. C. Dainty (Elsevier, Amsterdam, 1990), p. 37; T. Bellini, M. A. Glaser, N. A. Clark, and V. Degiorgio, *Phys. Rev. A* **44**, 5215 (1991).
  - [10] H. S. Carslaw and J. C. Jaeger, *Conduction of Heat in Solid* (Clarendon, Oxford, 1959), 2nd ed.
  - [11] J. Zhu, Ph.D. thesis, City University of New York, 1992.
  - [12] J. L. Lebowitz, *Phys. Rev. A* **133**, 895 (1964).
  - [13] C. W. J. Beenakker and P. Mazur, *Physica (Amsterdam)* **120A**, 388 (1983); **126A**, 349 (1984).
  - [14] C. W. J. Beenakker, *Physica (Amsterdam)* **128A**, 48 (1984).